

Short communication

# Formation of stable Cu<sub>2</sub>O from reduction of CuO nanoparticles

Jenna Pike<sup>a</sup>, Siu-Wai Chan<sup>a,\*</sup>, Feng Zhang<sup>a,1</sup>, Xianqin Wang<sup>b</sup>, Jonathan Hanson<sup>b</sup>

<sup>a</sup> Department of Applied Physics and Applied Mathematics, Columbia University, 200 S.W. Mudd Building,  
500 W. 120th St., New York, NY 10027, USA

<sup>b</sup> Chemistry Department, Brookhaven National Laboratory, Upton, NY 11973-5000, USA

Received 26 October 2005; received in revised form 26 January 2006; accepted 3 February 2006

Available online 10 March 2006

## Abstract

In situ time-resolved X-ray diffraction (TR-XRD) using synchrotron radiation has been used to capture the dynamics of the reduction of nanocrystalline CuO using a normal supply of CO gas. Copper(II) oxide nanoparticles 4–16 nm in width, as measured by XRD peak broadening, are synthesized using an aqueous organic-nitrate method and reduced in isothermal and temperature ramping reduction experiments. Temperature-programmed reduction of CuO nanoparticles using a ramping heating profile was observed to result in the sequential reduction process CuO → Cu<sub>2</sub>O → Cu, with CuO reducing completely to the intermediate Cu<sub>2</sub>O phase before further reduction to metallic copper. Isothermal reduction experiments at 250 °C show that CuO nanoparticles completely reduce to Cu<sub>2</sub>O, and this phase remains stable without further reduction with continued exposure to CO. In contrast to what is typically observed in bulk CuO in both isothermal and ramping reduction conditions, nanocrystalline CuO reduces to a stable Cu<sub>2</sub>O phase rather than forming metallic copper directly. The behavior of the CuO nanoparticles in temperature ramping reducing conditions is controlled by the particle size, with the smaller CuO nanoparticles exhibiting a greater stability and withstanding a higher temperature before their reduction to Cu<sub>2</sub>O and then to metallic copper nanoparticles.

© 2006 Elsevier B.V. All rights reserved.

**Keywords:** Copper oxide; Nanoparticles; Reduction of oxides; X-ray diffraction

## 1. Introduction

Copper(II) oxide is widely used as a catalyst because of its high activity and selectivity in oxidation and reduction reactions [1–3]. In particular, CuO was evaluated at one time as a possible alternative to precious metal catalysts such as platinum, palladium and rhodium for reactions involving H<sub>2</sub>, such as the oxidation of CO and hydrocarbons, and the reduction of NO<sub>x</sub> in automobile exhaust systems [1]. Copper oxide is used in the synthesis of methanol from CO and H<sub>2</sub>, and in the water-gas shift reaction (CO + H<sub>2</sub>O → CO<sub>2</sub> + H<sub>2</sub>) [4,5]. Other groups have reported the preparation of high purity, monodisperse nanocrystalline CuO using sonochemical preparation [6], microwave irradiation [7] and precipitation–pyrolysis [8], with particle sizes ranging from 4 nm [7] to

30 nm [8], and with both spherical [7,8] and acicular [6,8] morphologies.

Temperature-programmed reduction (TPR) studies of the reduction of bulk CuO have typically shown a direct transformation to Cu, without the formation of intermediate phases such as Cu<sub>2</sub>O or Cu<sub>4</sub>O<sub>3</sub> [2,9–12]. In several cases, Cu<sub>2</sub>O has been observed to form as an intermediate phase in the reduction of bulk CuO under conditions of decreased temperature and/or decreased oxygen partial pressure, and only as a transient species [2,7,12].

Copper(I) oxide, a p-type semiconductor with a direct bandgap of about 2.2 eV, has shown promise as a low-cost material for photovoltaic devices [13]. In addition to the applications of copper oxides in catalysis, a fundamental understanding of the Cu–O bonding is essential to the theory of high-temperature copper oxide superconductors [14].

In this study, we observe that nanocrystalline CuO undergoes a distinctly different reduction profile than that observed in bulk CuO. This report describes the use of in situ time-resolved X-ray diffraction (TR-XRD) to study the reduction of nanocrystalline CuO powders in 5% CO/He gas. Using high-intensity synchrotron radiation and rapid parallel data-collec-

\* Corresponding author. Tel.: +1 212 854 8519; fax: +1 212 854 8257.

E-mail addresses: [jmp2112@columbia.edu](mailto:jmp2112@columbia.edu) (J. Pike), [sc174@columbia.edu](mailto:sc174@columbia.edu) (S.-W. Chan), [feng.zhang@headway.com](mailto:feng.zhang@headway.com) (F. Zhang), [xiawang@bnl.gov](mailto:xiawang@bnl.gov) (X. Wang), [hanson1@bnl.gov](mailto:hanson1@bnl.gov) (J. Hanson).

<sup>1</sup> Present address: Headway Technologies, 678 S. Hillview Dr., Milpitas, CA 95035, USA.

tion devices, it is possible to detect trace intermediate phases and to monitor structural and chemical changes involved in catalytic reactivity [15]. In contrast to earlier observations in bulk CuO particles [12] and in our own experiments with bulk CuO powders, we have shown using in situ TR-XRD that nanocrystalline CuO reduces to Cu<sub>2</sub>O as a stable intermediate cubic phase, rather than undergoing a direct reduction to cubic copper.

## 2. Experimental

### 2.1. CuO nanoparticles preparation

We prepared nanocrystalline CuO powders by mixing together equal volumes of aqueous solutions of 0.004 M Cu(NO<sub>3</sub>)<sub>2</sub>·3H<sub>2</sub>O and hexamethylenetetramine (HMT) (0.25–1.5 M) at temperatures ranging from 36 to 50 °C. This method yields thin CuO rods, as determined from transmission electron microscopy (TEM). TEM was carried out using a JEOL JEM-100CX operated at 100 kV. The CuO nanoparticles were dispersed on carbon-coated copper grids for TEM analysis. All non-synchrotron X-ray diffraction experiments were performed using an Inel XRG 3000 diffractometer.

### 2.2. CuO nanoparticles characterization

Particle size was measured using the Scherrer equation,  $d = 0.941\lambda / (B \cos \theta_B)$ , where  $\lambda$  is the wavelength,  $B$  the full width at half maximum (FWHM) of the peak and  $\theta_B$  the Bragg angle. A correction was made for instrumental peak broadening by using the corresponding peaks in micron-sized powder (Aldrich). The ( $\bar{2}$ 02), (202) and ( $\bar{1}$ 13) peaks were used for particle size measurements.

### 2.3. Experimental set-up

The TR-XRD data were collected at beamline X7B at the National Synchrotron Light Source at Brookhaven National Lab ( $\lambda = 0.922$  Å). Diffraction patterns were collected using a MAR345 area detector at approximately 2 min intervals. The loose powders were loaded into an open sapphire capillary tube with an inner diameter of 0.5 mm. Quartz wool was inserted into each end to secure the sample position while gas flowed. One end of the capillary was connected to an inlet with a gas mixture of 5% CO and 95% He (99.999% purity), while the other end was connected to a flow meter. A flow rate of about 20 cm<sup>3</sup>/min was maintained throughout the process. The powder was heated with a kanthal wire that wrapped around the capillary. A thermocouple was inserted directly into the capillary near the sample to maintain accurate temperature during the measurements. In previous reports of bulk CuO reduction, TR-XRD experiments show that the formation of a transient, intermediate phase in the reduction of bulk CuO depends strongly on the reaction conditions [2,9,12].

Reduction experiments were conducted using either constant temperature (i.e. isothermal) or constant heating rate (i.e. ramping) temperature profiles. In the isothermal experiments,

the samples were heated from room temperature to 250 °C at a rate of 11 °C/min in 5% O<sub>2</sub>/He (99.99% purity) to prevent reduction due to burn-off of the organic used in synthesis before the sample reached final reduction temperature. The ramping experiments consisted of steadily increasing the temperature of nanocrystalline and bulk sample at a rate of 400 °C/h in flowing 5% CO/He gas.

## 3. Results and discussion

### 3.1. CuO nanoparticles characterization

Particle sizes ranged from 5 to 12 nm, depending on the reaction conditions, as measured by XRD. XRD of the as-made particles shows all CuO Bragg peaks. Particle size decreases as the concentration of the HMT solution increases, as can be seen by the broadening of the peaks in Fig. 1. As shown in Fig. 2(a), TEM images show acicular CuO nanoparticles. The copper oxide nanoparticles prepared by this method were pure CuO, as determined by XRD and TEM. These particles were stable and did not change in phase or size over a period of many months, as checked by XRD. Clusters of nanoparticles tend to form during TEM sample preparation. As a result, particles measured from TEM were larger in both width and length, and these measurements are larger than crystallite sizes obtained from XRD.

### 3.2. Reduction pathway

In situ TR-XRD using both isothermal and ramping temperature profiles shows that nanocrystalline CuO reduced to Cu<sub>2</sub>O in conditions that resulted in direct transformation to Cu when reducing bulk CuO. Figure 3 illustrates the two different reduction pathways observed in bulk and nanoscale CuO. Bulk CuO normally follows a single step reduction, as in pathway 1, while Fig. 2(a and b) describe the step-wise reduction observed in

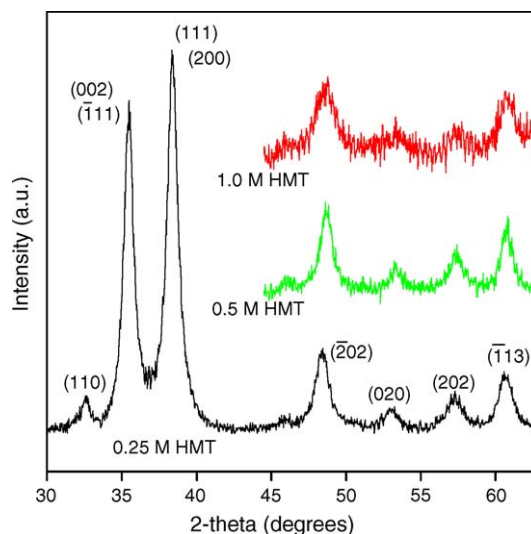
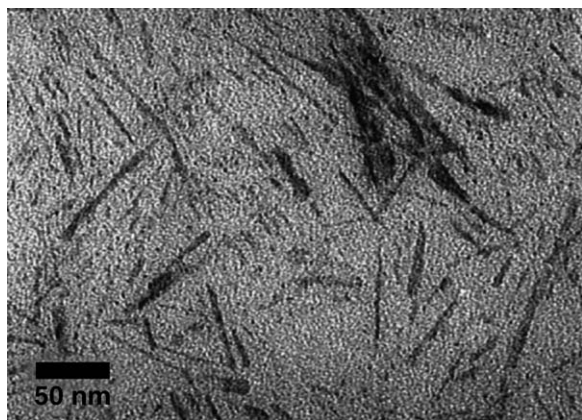
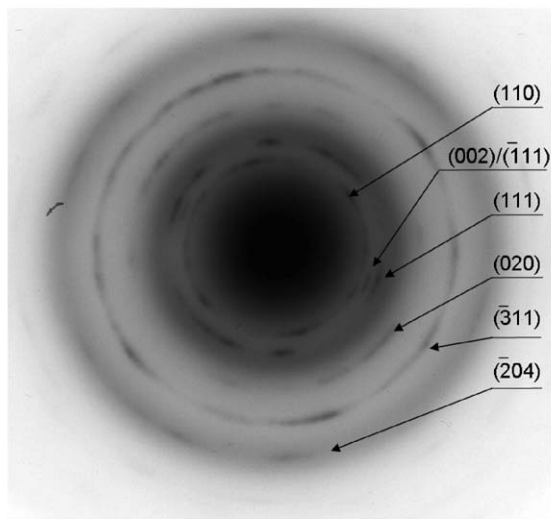


Fig. 1. X-ray diffraction patterns of CuO nanoparticles synthesized using 0.004 M Cu(NO<sub>3</sub>)<sub>2</sub> concentration at 50 °C for 30 min, with HMT concentration increasing from 0.25 to 1.0 M. A trend of decreasing particle size with increase in HMT concentration is evident from the peak width broadening.



(a)



(b)

Fig. 2. TEM shows acicular CuO particles synthesized with 1.0 M HMT (a). CuO nanoparticles aggregate into clusters, resulting in the appearance of particles of varying thicknesses and lengths, and larger particle sizes than those measured from TEM. Selected area diffraction (b) shows diffraction from the planes, from center, (1 1 0), (0 0 2)/(1 1 1), (1 1 1), (0 2 0), (3 1 1) and (2 0 4).

the reduction of CuO nanoparticles, from the monoclinic CuO, to cubic Cu<sub>2</sub>O, and further reduction to face centered cubic Cu.

### 3.3. Isothermal reduction

Results of isothermal reduction are given in the first section of Table 1. At 250 °C, 11 nm CuO nanoparticles reduced completely to Cu<sub>2</sub>O within 10 min, as shown in Fig. 4. The

Table 1  
Formation of products in isothermal and ramping CuO reduction experiments

Heating profile	Initial CuO particle size	Cu <sub>2</sub> O formation	Cu formation (°C)
Isothermal (250 °C)	11 nm	10 min	–
Ramping (400 °C/h)	5 nm	240 °C	450
	12 nm	190 °C	360
	Microns (bulk)	–	150

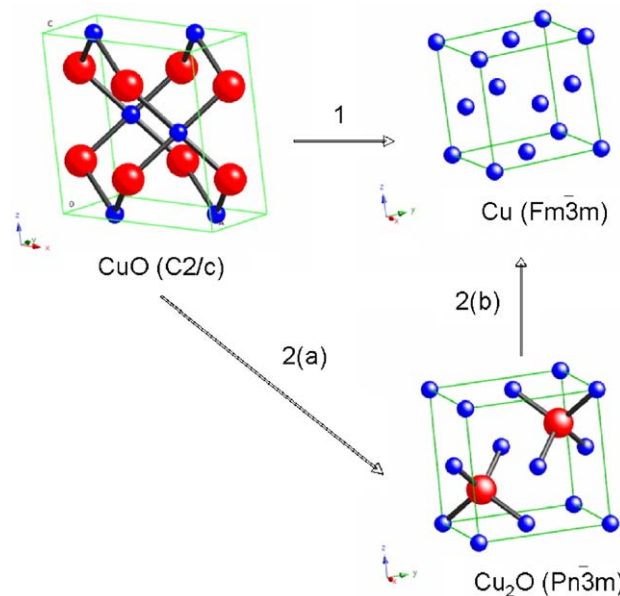


Fig. 3. Bulk CuO typically reduces directly to metallic Cu, as indicated in pathway 1. Nanoscale CuO follows the two-step reduction pathway, reducing first to Cu<sub>2</sub>O, as in pathway Fig. 2(a), then to Cu by pathway Fig. 2(b) under nearly identical conditions. Space groups are indicated for CuO, Cu<sub>2</sub>O and Cu.

Cu<sub>2</sub>O phase was stable with continued holding at 250 °C. Additional isothermal experiments at 250 °C using 5 and 14 nm CuO nanoparticles showed similar results: immediate reduction to Cu<sub>2</sub>O and no further reduction for up to 45 min.

### 3.4. Ramping temperature reduction

Reduction of bulk CuO directly to metallic Cu began at 150 °C and was complete at 270 °C, whereas nanocrystalline

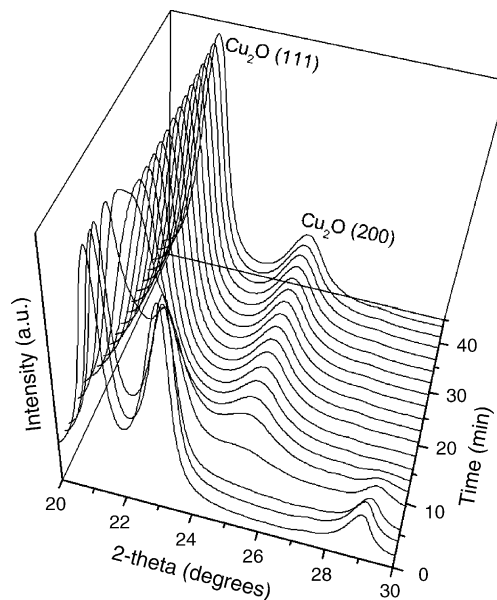


Fig. 4. Time-resolved XRD data during the isothermal reduction of nanocrystalline CuO (11 nm) under a 5% CO/95% He mixture (flow rate ~ 20 cm<sup>3</sup>/min) at 250 °C. CuO completely reduces to stable Cu<sub>2</sub>O phase with no trace of metallic Cu present after 45 min.

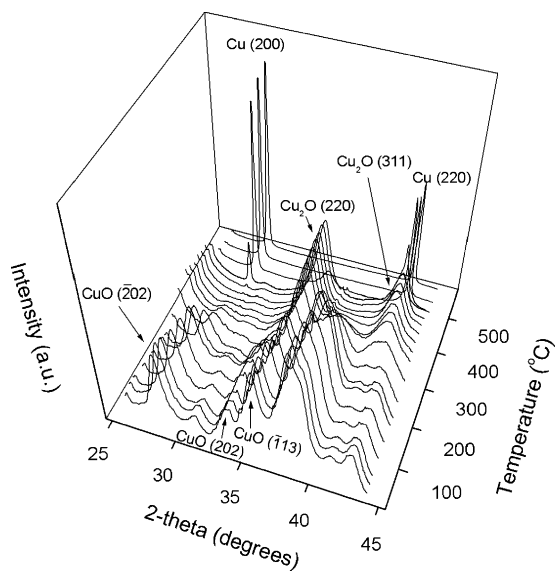


Fig. 5. Time-resolved XRD data obtained in the ramping reduction of 5 nm CuO nanoparticles under a 5% CO/95% He mixture (flow rate  $\sim 20 \text{ cm}^3/\text{min}$ ) with  $400 \text{ }^\circ\text{C}/\text{h}$  heating rate. CuO reduced to  $\text{Cu}_2\text{O}$  at  $250 \text{ }^\circ\text{C}$ , with further reduction to Cu beginning at  $450 \text{ }^\circ\text{C}$ .

CuO followed a two-step reduction process, completely reducing first to  $\text{Cu}_2\text{O}$ , then to Cu in ramping temperature experiments. Nanocrystalline CuO reduced first to  $\text{Cu}_2\text{O}$ , then to Cu, as shown in Fig. 5 (5 nm CuO particles) and Fig. 6 (12 nm CuO particles). As indicated in Table 1, reduction to  $\text{Cu}_2\text{O}$  began at  $190 \text{ }^\circ\text{C}$  for 12 nm particles and further reduction to Cu began at  $360 \text{ }^\circ\text{C}$ . Initial reduction of 5 nm CuO particles to  $\text{Cu}_2\text{O}$  occurred at  $240 \text{ }^\circ\text{C}$ , with formation of Cu beginning at  $450 \text{ }^\circ\text{C}$ , with the same ramping rate.

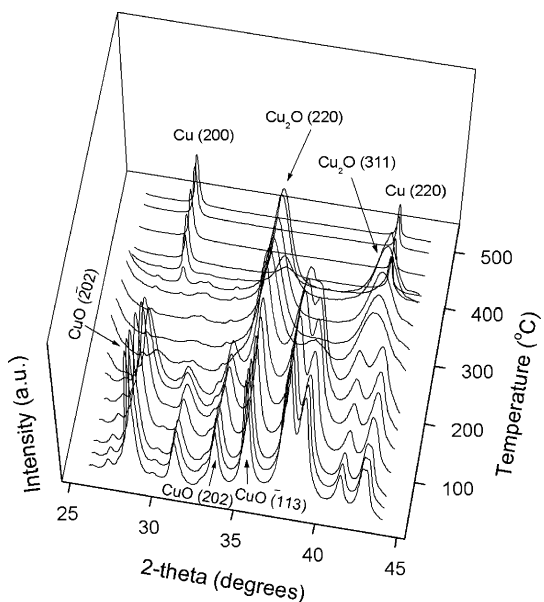


Fig. 6. Time-resolved XRD data obtained in the ramping reduction of 12 nm CuO nanoparticles under a 5% CO/95% He mixture (flow rate  $\sim 20 \text{ cm}^3/\text{min}$ ) with  $400 \text{ }^\circ\text{C}/\text{h}$  heating rate. CuO reduced to  $\text{Cu}_2\text{O}$  at  $190 \text{ }^\circ\text{C}$ , with further reduction to Cu beginning at  $390 \text{ }^\circ\text{C}$ .

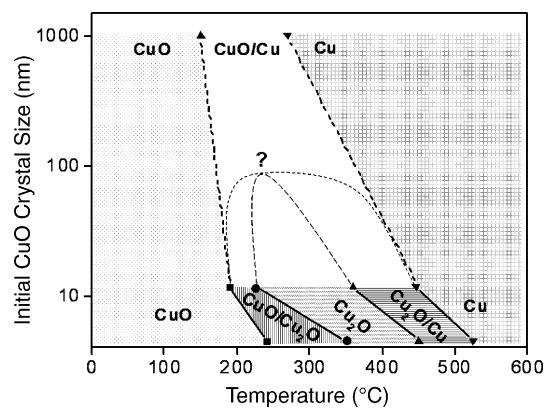


Fig. 7. In ramping experiments with  $400 \text{ }^\circ\text{C}/\text{h}$  heating rate, in 5% CO/He (flow rate  $\sim 20 \text{ cm}^3/\text{min}$ ), 5 and 12 nm CuO particles reduce first to  $\text{Cu}_2\text{O}$ , then to Cu as temperature increases further. As initial CuO particle size increases, the temperature at which reduction begins decreases. In the unshaded region, a phase boundary is suggested for particles larger than 12 nm, but smaller than bulk ( $\sim 1000 \text{ nm}$ ). Dashed lines indicate suggested phase boundaries, while solid lines connect data points of relatively similar particle size. The question mark indicates a possible, critical maximum for the initial CuO particle size that will reduce to  $\text{Cu}_2\text{O}$ .

Although kinetics are faster in nanoscale, our experiments show that reduction occurs at a higher temperature, or more reluctantly, as CuO particle size decreases, suggesting that other factors are controlling reduction rate. The formation of the  $\text{Cu}_2\text{O}$  intermediate phase also occurs at increased temperature as the initial CuO particle size decreases. The results of the three temperature ramping experiments described in this paper are compiled in Fig. 7, which illustrates the size-dependence of the reduction behavior, under the same heating rate.

In both the ramping and isothermal reduction experiments, CuO nanoparticles reduced completely to  $\text{Cu}_2\text{O}$ . No further reduction occurred within 45 min in the isothermal experiments at  $250 \text{ }^\circ\text{C}$ . In temperature ramping experiments, reduction to  $\text{Cu}_2\text{O}$  began at  $190 \text{ }^\circ\text{C}$  for 12 nm particles, with further heating resulting in complete reduction of the  $\text{Cu}_2\text{O}$  to metallic Cu. Changes in the ramping rate are expected to result in a shift of the reduction temperatures. Unlike the reduction of bulk CuO to  $\text{Cu}_2\text{O}$ , which depends strongly on reaction conditions [2,9,12], the formation of  $\text{Cu}_2\text{O}$  from CuO nanoparticles shows a greater dependence on initial particle size. We expect that there is a critical particle size, above which direct reduction occurs, and below which sequential reduction takes place.

#### 4. Conclusions

Copper oxide nanoparticles ranging from 5 to 12 nm exhibit reduction behavior that is significantly different from that of bulk CuO. CuO nanoparticles form a stable  $\text{Cu}_2\text{O}$  intermediate phase under reducing conditions that do not result in the appearance of  $\text{Cu}_2\text{O}$  as an intermediate phase in the reduction of bulk CuO material. In isothermal experiments at  $250 \text{ }^\circ\text{C}$ , CuO nanoparticles reduced completely to

Cu<sub>2</sub>O, with no further reduction. In ramping experiments, the temperature at which new reduced phases (Cu<sub>2</sub>O, CuO) appear increases as the initial CuO particle size decreases. Clearly, factors other than diffusion kinetics play a significant role in reduction of CuO nanoparticles. Cu<sub>2</sub>O has shown higher catalytic activity in the splitting of water to O<sub>2</sub> and H<sub>2</sub> [16] and has also shown greater catalytic activity than CuO in the oxidation of CO [17]. Greater control over the formation of Cu<sub>2</sub>O nanoparticles in reducing conditions may have important implications in the use of the copper oxide system in catalytic applications.

### Acknowledgements

This work was primarily supported by the MRSEC program of the National Science Foundation under Award No. DMR-0213574.

This work was partially supported by Track 2, GK12: Technology Integration Partnership: Bringing Emerging STEM Research into Grades 5–12 enabled by New Technologies (NSF award 0338329).

The work done at BNL was supported by U.S. Department of Energy Division of Chemical Sciences, Office of Basic Energy Sciences under contract no. DE-AC02-98CH10886. The NSLS is supported by the Divisions of Chemical and Materials Science of the Department of Energy.

### References

- [1] J.T. Kummer, *Prog. Energy Combust. Sci.* 6 (1980) 177–199.
- [2] J.A. Rodriguez, J.Y. Kim, J.C. Hanson, M. Pérez, A. Frenkel, *Catal. Lett.* 85 (2003) 247–254.
- [3] J.-L. Li, T. Takeguchi, T. Inui, *Appl. Catal. A* 139 (1996) 97–106.
- [4] C.T. Campbell, K.A. Daube, *J. Catal.* 104 (1987) 109–119.
- [5] E. Colbourn, R.A. Hadden, H.D. Vandervell, K.C. Waugh, G. Webb, *J. Catal.* 130 (1991) 514–527.
- [6] R.V. Kumar, R.E. Elgamiel, Y. Diamant, A. Gedanken, *Langmuir* 17 (2001) 1406–1410.
- [7] H.W. Wang, J.Z. Xu, J.J. Zhu, H.Y. Chen, *J. Cryst. Growth* 224 (2002) 88–94.
- [8] H. Fan, L. Yang, W. Hua, X. Wu, Z. Wu, S. Xie, B. Zou, *Nanotechnology* 15 (2004) 37–42.
- [9] J.Y. Kim, J.A. Rodriguez, J.C. Hanson, A.I. Frenkel, P.L. Lee, *J. Am. Chem. Soc.* 125 (2003) 10684–10692.
- [10] T.L. Reitz, P.L. Lee, K.F. Czaplewski, J.C. Lang, K.E. Popp, H.H. Kung, *J. Catal.* 199 (2001) 193–201.
- [11] B.S. Clausen, H. Topsøe, *Catal. Today* 9 (1991) 189–196.
- [12] X. Wang, J.C. Hanson, A.I. Frenkel, J.-Y. Kim, J.A. Rodriguez, *J. Phys. Chem. B* 108 (2004) 13667–13673.
- [13] M. Yin, C.-K. Wu, Y. Lou, C. Burda, J.T. Koberstein, Y. Zhu, S. O'Brien, *J. Am. Chem. Soc.* 127 (2005) 9506–9511.
- [14] J.M. Zuo, M. Kim, M. O'Keefe, J.C.H. Spence, *Nature* 401 (1999) 49–52.
- [15] P. Norby, J.C. Hanson, *Catal. Today* 39 (1998) 301–309.
- [16] S. Ikeda, T. Takata, T. Kondo, G. Hitoki, M. Hara, J.N. Kondo, K. Domen, H. Hosono, H. Kawazoe, A. Tanaka, *Chem. Commun.* 20 (1998) 2185–2186.
- [17] G.G. Jernigan, G.A. Somorjai, *J. Catal.* 147 (1994) 567–577.